J Electr Eng Technol Vol. 9, No. 6: 2004-2012, 2014
http://dx.doi.org/10.5370/JEET.2014.9.6.2004

ISSN(Print) 1975-0102
ISSN(Online) 2093-7423

Dynamic Analysis and Controller Design for Standalone Operation of Photovoltaic Power Conditioners with Energy Storage

Sun-Jae Park*, Jong-Hyun Shin*, Joung-Hu Park† and Hee-Jong Jeon*

Abstract – Energy storage devices are necessary to obtain stable utilization of renewable energy sources. When black-out occurs, distributed renewable power sources with energy storage devices can operate under standalone mode as uninterruptable power supply. This paper proposes a dynamic response analysis with small-signal modeling for the standalone operation of a photovoltaic power generation system that includes a bidirectional charger/discharger with a battery. Furthermore, it proposes a DC-link voltage controller design of the entire power conditioning system, using the storage current under standalone operation. The purpose of this controller is to guarantee the stable operation of the renewable source and the storage subsystem, with the power conversion of a very efficient bypass-type PCS. This paper presents the operating principle and design guidelines of the proposed scheme, along with performance analysis and simulation. Finally, a hardware prototype of 1-kW power conditioning system with an energy storage device is implemented, for experimental verification of the proposed converter system.

Keywords: Standalone, Photovoltaic power generator, Energy storage, Power conditioner, Dynamic response model, Small-signal model, Controller design

1. Introduction

The need for renewable energy sources has become more important than ever before, due to the depletion of fossil fuel, and its serious impact on environmental contamination. Renewable energy sources are starting to be used in residential applications, as well as in commercial buildings and engineering industries [1]. Therefore, many renewable energy sources have been actively studied, such as solar energy and wind power systems. However, the power output from renewable energy sources is determined by environmental circumstances; hence net power generation fluctuates according to the weather variation, and the normal operation has also been restricted to specific conditions [2-3]. For these reasons, the demand for energy storage devices that accompany renewable energy systems has been increasing, in order to stably use renewable energy sources [4].

When these sources generate insufficient output power, a storage device can relieve the energy shortage of the load [5]. On the other hand, when the amount of output power from the renewable sources exceeds the consumption of the load, the storage device can store the excess energy. This storage concept allows us to use power generation from uncontrollable energy sources in an efficient and stable manner [6-7].

In general, power conditioning systems with energy storage include a charger / discharger that can charge / discharge the storage device, as well as a two-stage power converter that provides the energy to local loads, or to the power grid [8-10]. A charger/discharger can be connected to the output of a renewable energy source, or the DC-link, to stabilize the power generation [11-13]. Figs. 1 and 2 show conventional circuits of the power conditioning systems, including an energy storage device and a renewable source. Fig. 1 is a conventional scheme that attaches a charger/discharger at the output of the renewable energy source. This circuit has a drawback that the power capacity for the boost converter design is greater than the peak power of the source. Also, the power efficiency decreases significantly, since the discharging energy must pass through the two conversion stages of the discharger

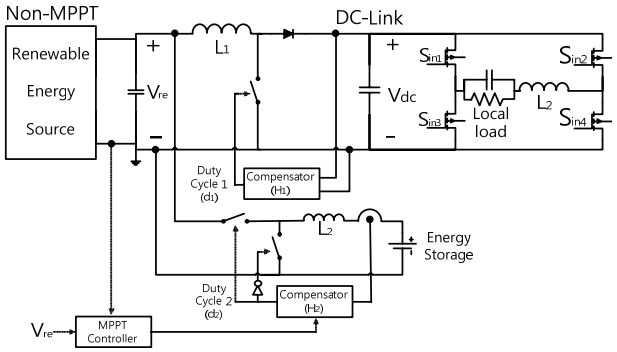

Fig. 1. Conventional Architecture of the power conditioning system with a renewable energy source and an energy storage device under standalone operation (source-connection) [22]

† Corresponding Author: Dept. of Electrical Engineering, Soongsil University, Korea. (wait4u@ssu.ac.kr)
* Dept. of Electrical Engineering, Soongsil University, Korea. (koske1983@hanmail.net, shin3082@naver.com, hjjeon@ssu.ac.kr)
Received: March 7, 2014; Accepted: July 5, 2014

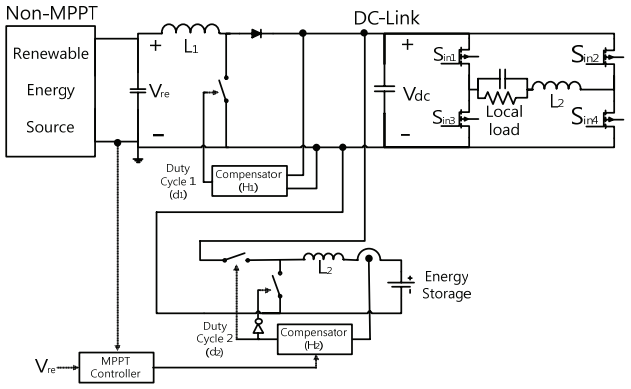

Fig. 2. Conventional Architecture of the power conditioning system with a renewable energy source and an energy storage device under standalone operation (DC-link connection) [22]

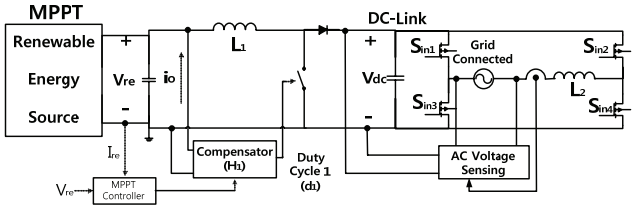

Fig. 3. Cascaded two-stage power conditioning system with a renewable source under grid-connected operation [22]

and the boost converter in series. Fig. 2 is another scheme that attaches the charger/discharger at the DC-link rail [14-16]. Power efficiency decreases significantly, due to the fact that the charging current must pass through the boost converter and the charger [17-18]. Also, since the AC voltage of the post-stage inverter is not fixed under standalone mode, the controller of the boost converter, or of the energy storage sub-system must control the DC-Link voltage. Actually, analysis and design methods for the maximum-power tracking control of the renewable source and the dc-link in the cases of Figs. 1 and 2, have rarely been reported. On the other hand, power conditioning systems with grid-connection typically implement maximum power point tracking (MPPT) controllers for renewable energy sources, because the AC voltage of the grid-connected mode is regulated by the grid, as shown in Fig. 3.

In this paper, a new standalone controller design for a bypass charger/discharger scheme is proposed, in order to improve the conversion efficiency in a photovoltaic power system. The bypass scheme is shown in Fig. 4, which shortens the conduction path, due to the different charging and discharging power paths. This skips the redundant power process of the boost converter inserted in the charging path of the normal (grid-connection) mode and in the discharging path, as an uninterruptible power supply (UPS) [19-21]. When blackout occurs, the power conditioning system starts to operate under standalone mode, as an UPS. Then, the post-stage inverter regulates

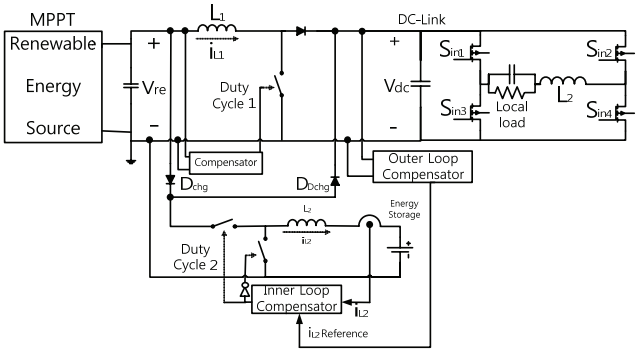

Fig. 4. Proposed control architecture of the power conditioning system with a renewable energy source and an energy storage device under Standalone operation. The DC-link is regulated by the storage current and MPPT is done by the boost converter as shown in Fig. 3.

the AC output voltage within the normal operating range; and also, the first-stage boost converter controls the operating point of the renewable source according to the maximum power point tracking algorithm, to prevent degradation of the generation efficiency. An energy storage device is introduced into the system for the DC-link regulation, which interfaces through the charger/discharger. One more control freedom from the energy buffer enables the maintenance of the DC-link voltage at a high enough level for the achievement of a step-down power stream of the full-bridge inverter. With the help of the DC-link voltage regulation from the storage sub-system, the control architecture of the boost converter needs no alteration, under mode changes between grid-connection and standalone. If the application were to be extended to grid-connection, the storage could also attenuate the power fluctuation of the renewable energy sources, which fluctuation should be avoided for the stable operation of a conservatively regulated power grid. However, there are no special challenges in the controller design for the grid-connection of the bypass PCS, as mentioned in [22].

This paper presents the operating principle and controller design guidelines of the proposed standalone control scheme, along with the dynamic response analysis based on the small signal modeling, including the energy storage device. Numerical analysis using the simulation software PSIM is also included, to verify the model. Finally, a 1 kW hardware prototype of the power conditioning system with the energy storage device is implemented, for experimental verification of the proposed power conditioning systems analysis and design guidelines.

2. Dynamic Response Model

2.1 System configuration

The proposed controller configuration of the standalone

renewable-energy system, which consists of a renewable energy source and an energy storage device interfacing through a power conditioning system, is shown in Fig. 4. The first stage of the power conditioner has a voltage feedback loop to control the renewable source operation, and the post stage inverter has an output voltage loop, to maintain the AC output [23-24]. The bi-directional buck-boost charger in the storage sub-system includes a current-mode controller to regulate the inductor current, performing power-flow control of the energy storage device. In this paper, a stack of super-capacitors is considered as the storage device, because a fast charging / discharging dynamic response is required for the controller test of the entire system. The power conditioning system (PCS) in the figure has a different conduction path between the charging and discharging mode. Figs. 5 and 6 show the bypassed power flow of the PCS under the charging and discharging mode, respectively. As shown in Fig. 5, during the charging mode, the charger/discharger directly charges the storage device from the renewable source through a conduction diode (D_{Chg}). During the operation, the outer loop voltage controller that is in charge of the DC-link voltage regulation directs the inner-loop current

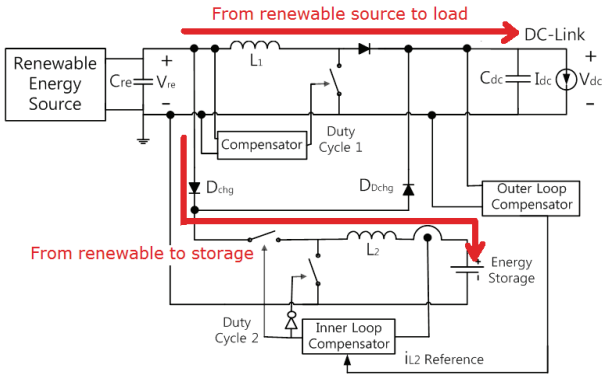

Fig. 5. Bypassed power flow of the PCS with a renewable energy source and an energy storage device under charging mode [22]

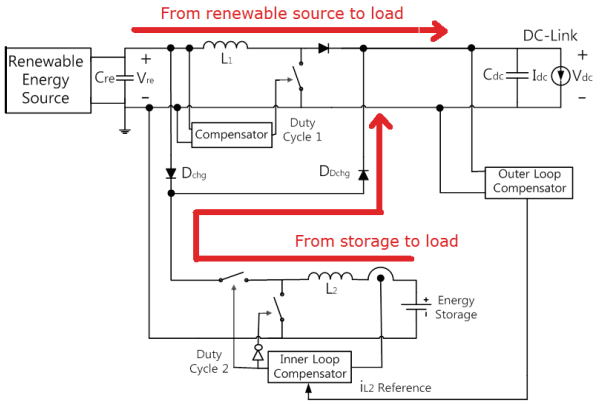

Fig. 6. Bypassed power flow of the PCS with a renewable energy source and an energy storage device under discharging mode [22]

controller. From the control architecture, the PCS constantly regulates the DC-link, while charging the storage by the extra energy from the renewable source.

During the discharging mode, the bidirectional converter directly discharges the storage device to the DC-link, through the other diode (D_{Dchg}) naturally conducting by the negative current flow, as shown in Fig. 6. During the operation, likewise during charging, the inner-loop current controller is directed by the outer loop voltage controller, and the PCS constantly regulates the DC-link with the discharging current from the storage.

Through the bypassing path, energy can be stored and released more efficiently, significantly reducing the conversion loss [22]. The boost converter's power capacity is also the same as the maximum power of the source, due to the bypass of the charging/discharging energy of the storage device. The scheme is still cost-competitive, and offers a low layout burden, because of the small part count increase of the two extra diodes for the bypass [22]. However, since the first-stage boost converter in the main power stream simultaneously operates with the converter of the storage sub-system, as mentioned above, the three controller design of the entire PCS for the standalone operation necessarily has to consider their dynamic interaction, which seems quite complicated. For stable controller design, the individual small-signal models of the subsystems are first derived; and then, the interaction analysis between the systems is performed.

The following sections present the small-signal analysis for investigating the dynamic response of the bypass power conditioning system, and the design results of the standalone operation. Since the equivalent circuit under discharging mode is simple, and the controller design is quite straightforward, only the charging mode will be considered for the analysis and design.

2.2 Small-signal analysis

The boost converter of the main power conditioning system controls the output voltage of the renewable energy source to perform MPPT operation, and the full-bridge inverter provides AC voltage within normal operating range for the local load, on the condition that the DC-link voltage is regulated high enough for the inverter. Thus in the proposed scheme, the DC-link voltage is consistently regulated by the charger/discharger's controller, composing an outer voltage-feedback control loop. For the voltage control, power delivery to the inverter matches the power consumption of the local load, through power compensation of the energy storage device. The inductor-current controller performs the compensation, under the voltage controller of the storage subsystem. If the renewable power generation is greater than the load, then the surplus energy flows directly to the storage in the charging mode of the bi-directional converter under the current control. Otherwise, the controller uses the converter for power release from the

storage to the inverter through the short-cut path, with the amount of energy exactly the same as that required for the voltage regulation. If the voltage of the energy storage is always lower than the voltage (V_{re}) of the renewable source, the bi-directional converter can be unified into single circuit topology. This paper employs one of the simplest bi-directional topologies, that of a buck / boost converter.

The following subsections describe the small-signal modeling and dynamic response analysis of the charger / discharger and boost converter with a photovoltaic energy source for the controller design.

2.2.1 Control-to-output transfer function and an output impedance of the boost converter under charging mode

While charging energy from the renewable energy source to the energy storage device, the charger/discharger is in electric contact with the output of the renewable energy source. Hence, to design the inner current compensator of the charger/discharger, the output impedance of the boost converter with the renewable energy source must first be considered.

First, the open-loop control-to-output (G_{Vred1}) of the boost converter with the renewable energy source must be derived, to design the compensator (H1) of the boost converter. Fig. 7 is the simplified equivalent circuit of the closed-loop boost converter with the renewable energy source, for deriving the output impedance from the storage subsystem [22]. At this time, the equivalent circuit model replaces the renewable energy source, to use the state-space averaging technique to derive the small-signal model. Eq. (1) is the control-to-renewable voltage transfer function of the open-loop boost converter.

$$G_{V_{re}d_1} = \frac{\hat{v}_{re}}{\hat{d}_1} = -\frac{\frac{D_1'^2 I_{L_1}}{A_{C_{dc}}} + V_{dc}}{Z_{L_1}A_{C_{re}} + 1 + \frac{D_1'^2 A_{C_{re}}}{A_{C_{dc}}}} \quad (1)$$

$$\begin{pmatrix} Z_{L_1} = sL_1 + r_{esr1} \\ A_{C_{re}} = sC_{re} + \frac{1}{r_{re}} \\ A_{C_{dc}} = sC_{dc} \\ D_1' = 1 - D_1 \end{pmatrix}$$

where, V_{dc} is the DC-link voltage, I_{L1} is the boost inductor current, and r_{esr1} is the equivalent series resistance of the inductor.

Then, the voltage compensator of the boost converter is designed with a linear equation, such as the PI compensator shown in (2). The PI compensator is considered in this paper, as a design example for each of the compensators. Also, other peripheral transfer functions, such as the sensing gain, sampling effect, and PWM gain in the loop, are supposed as unity in the loop design.

For derivation of the closed-loop output impedance, the open-loop output impedance of the boost converter with the renewable energy source is derived as Eq. (3), by using a state-space averaging technique.

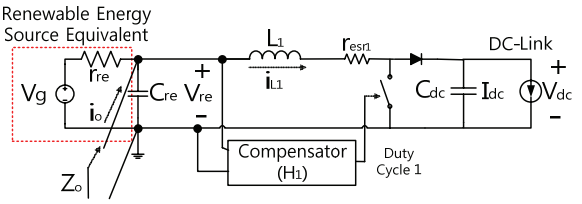

Fig. 7. Equivalent circuit of the closed-loop boost converter with a photovoltaic energy source to find the output impedance at the joint with energy storage subsystem.

$$Z_{o\cdot Open\ Loop} = \frac{\hat{v}_{re}}{\hat{i}_o} = \frac{Z_{L_1} + \frac{D_1'^2}{A_{C_{dc}}}}{Z_{L_1}A_{C_{re}} + 1 + \frac{D_1'^2 A_{C_{re}}}{A_{C_{dc}}}} \quad (3)$$

Finally, the closed-loop output impedance ($Z_{o.Closed}$) of the boost converter with the renewable energy source can be derived as Eq. (4).

$$Z_{o.Closed\ Loop} = \frac{Z_{o.open}}{1 + T_1} \quad (4)$$

$$\left(T_1 : Loop\ gain\ of\ the\ boost\ converter\ \left(= G_{v_{re}d_1}H_1\right)\right)$$

The output impedance represents the dynamic interaction of the boost converter with the energy storage system.

2.2.2 Control-to-output transfer function and controller design of the charger/discharger

From the results of the previous derivation, the equivalent small signal model of the energy storage subsystem with the interaction of the boost converter can be drawn, as in Fig. 8. From the figure, the transfer function of the charger / discharger (G_{iL2d2}), along with the dynamic interaction of the boost converter ($Z_{o.Closed}$), is derived as Eq. (5).

$$G_{i_{L_2}d_2} = \frac{\hat{i}_{L_2}}{\hat{d}_2} = \frac{V_{re} - D_2 I_{L_2} Z_{o.Closed}}{Z_{L_2}} \quad (5)$$

$$\left(Z_{L_2} = sL_2 + r_{esr2}\right)$$

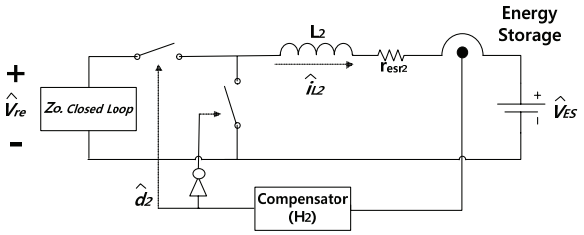

Fig. 8. Small signal model of the charger / discharger including the interaction (output impedance) of the boost converter

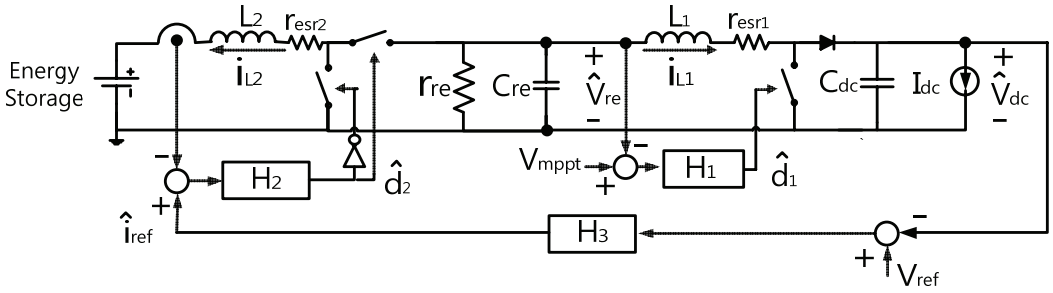

Fig. 9. Entire control scheme diagram of the renewable-sourced power conditioning system with energy storage including the charger/discharger under the charging mode

In the equation, it can be seen that as the output impedance increases, the transfer function of the charger deviates more from the function, without considering the interaction.

Finally, the current loop gain (T_2) of the charger can be derived as Eq. (6), using the transfer function in Eq. (5).

$$T_2 = G_{i_{L_2} d_2} H_2 \tag{6}$$

2.2.3 Outer loop design of the charger/discharger

As shown in Fig. 9, the outer-loop compensator of the charger / discharger controls the DC-link voltage in standalone operating mode. Fig. 10 shows the small-signal block diagram of the entire PCS, to finally include the outer-loop compensator H_3 of the system shown in Fig. 9. From the block diagram, it can be seen that the outer-loop controller design of the charger/discharger needs the derivation of the sub-functions G_{vdcvre}, G_{vred2}, G_{iL2d2} and G_{vdcd1}.

First, from consideration of the interaction ($Z_{in,Closed\ Loop}$), the audio-susceptibility (G_{vdcvre}) of the boost converter can be derived:

$$G_{V_{dc}V_{re}} = \frac{\hat{v}_{dc}}{\hat{v}_{re}} = \frac{D_1'}{A C_{dc} Z_{L_1} + D_1'^2} \tag{7}$$

Second, the transfer function (G_{vdcd1}) of control-to-DC-link voltage in the boost converter can be derived as Eq. (8).

$$G_{V_{dc}d_1} = \frac{\hat{v}_{dc}}{\hat{d}_1} = \frac{D_1' V_{dc} - I_{L_1} Z_{L_1}}{A C_{dc} Z_{L_1} + D_1'^2} \tag{8}$$

Third, the transfer function (G_{vred2}) of control-to-voltage of the renewable source in the charger/discharger can be derived as Eq. (9).

$$G_{V_{re}d_2} = \frac{\hat{v}_{re}}{\hat{d}_2} = -\frac{(D_2 V_{re} + I_{L2} Z_{L_2}) Z_{o\text{-}Closed\ Loop}}{Z_{L_2} + D_2^2 Z_{o\text{-}Closed\ Loop}} \tag{9}$$

Fourth, the transfer function ($G_{vreiref}$) of the current reference to voltage of the renewable source in the charger/discharger can be derived as Eq. (10).

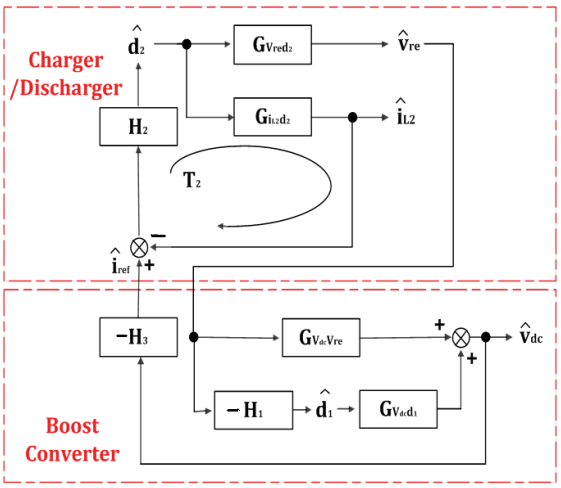

$G_{v_{re}d_2}$: transfer function of control to voltage of the renewable source in the charger

$G_{i_{L_2}d_2}$: transfer function of control to inductor current in the charger

$G_{V_{dc}V_{re}}$: Audiosusceptibility of the renewable to DC – link voltage

$G_{V_{dc}d_1}$: transfer function of control to DC – link voltage in boost

Fig. 10. Small-signal block diagram of the entire power conditioning system at charging mode.

$$G_{v_{re}i_{ref}} = \frac{\hat{v}_{re}}{\hat{i}_{ref}} = \frac{H_2 G_{vre\,d2}}{1 + T_2} \tag{10}$$

Fifth, the transfer function ($G_{vdciref}$) of the current reference to DC-link voltage in charger/discharger can be established as Eq. (11).

$$G_{v_{dc}i_{ref}} = \frac{\hat{v}_{dc}}{\hat{i}_{ref}} = G_{v_{re}i_{ref}} \left(G_{V_{dc}V_{re}} - H_1 G_{V_{dc}d_1} \right) \tag{11}$$

Finally, the outer loop gain (T3) of the total power conditioning system, including the dynamic interaction between the main power stream and energy storage subsystem, can be derived as Eq. (12).

$$T_3 = G_{v_{dc}i_{ref}} \cdot H_3 \tag{12}$$

where, H_3 is the compensa tor of the outer voltage loop.

3. Simulation Results

This section verifies previous derivation results by comparison between frequency responses of the symbolic closed-form analysis, based on the transfer functions of the state-space averaged model in previous sections, and those of the numerical analysis through PSIM simulation, based on the exact PWM switching-circuit model. The Bode plot of the averaged-model transfer function is drawn by MATLAB software. The dynamic interaction between the main power stage and the energy storage subsystem can be seen from the simulation results of the proposed renewable energy system; and also, each controller of the system is designed based on the Bode plot. Finally, the control stability is proved, by checking the phase margin of the feedback control loop. The key parameters of the simulation and hardware experiment are shown in Table 1.

To investigate the dynamic interaction of the boost converter with the charger/discharger, the frequency response of the closed-loop output impedance ($Z_{o.Closed}$) of the boost converter is first analyzed, as shown in Fig. 11. From the figure, it can be seen that the derived equation of the interaction matches the exact model simulation well, and the interaction is maximized around the 100Hz range. The transfer function and the controller of the charger can be analyzed, using the response plot. As shown in Fig. 12, the phase margin of the charger's current loop gain (T2) employing the design example of the compensator is about 75°, which results in good stability.

As shown in Fig. 10, the transfer function ($G_{vdciref}$) is derived, along with the sub-transfer functions of G_{vdcvre}, G_{vred2}, G_{iL2d2} and G_{vdcd1}, in order to design the DC-link voltage-feedback controller of the power conditioner, including the dynamic interaction of the boost converter.

Fig. 13 shows the frequency response of the transfer

Table 1. Element data

V_g	300V	V_{dc}	320V
V_{re}	150V	V_{ES}	50V
r_{re}	45Ω	I_{dc}	1.5A
L_1	1.4mH	L_2	1.4mH
C_{re}	2200μF	C_{dc}	6800μF
r_{esr1}	0.3Ω	r_{esr2}	0.3Ω
D_1	0.53125	D_2	0.46875
K_{p2}	0.0005	K_{i2}	120.5
K_{p2}	0.05	K_{i2}	2000
K_{p2}	1	K_{i2}	20

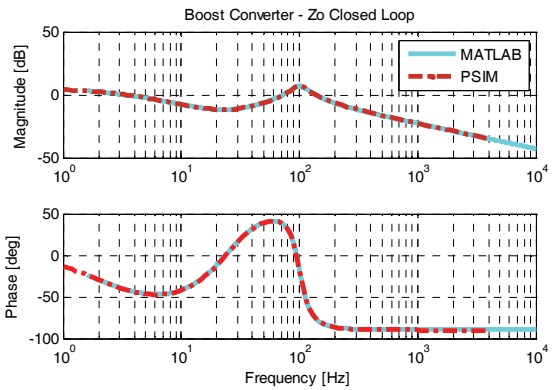

Fig. 11. Closed-loop output impedance ($Z_{o.closed}$) of the boost converter including the renewable energy source. (Solid: analytic, dotted: numerical result)

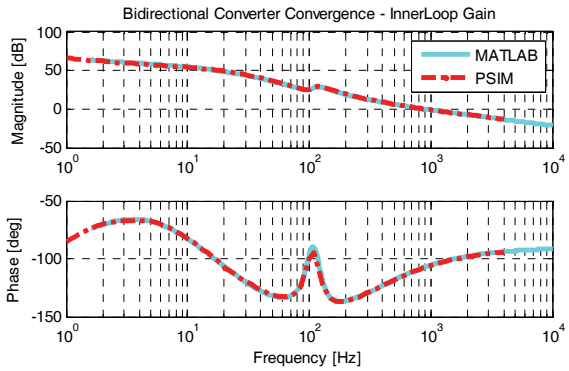

Fig. 12. Inner-Loop Gain (T2) of the charger/discharger, including dynamic interaction of the boost converter with the renewable energy source (Solid: analytic, dotted: numerical result)

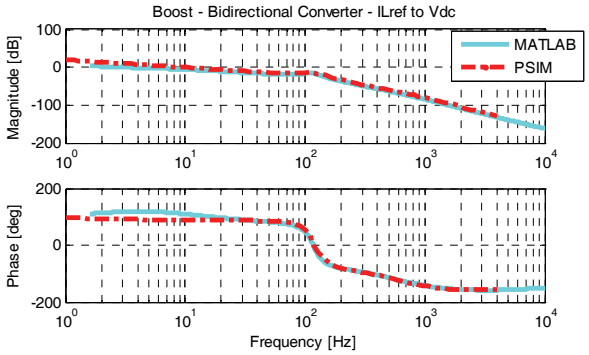

Fig. 13. Transfer function ($G_{vdciref}$) including inductor-current control loop of the charger / discharger, as well as the dynamic interaction of the boost converter (Solid: analytic, dotted: numerical result)

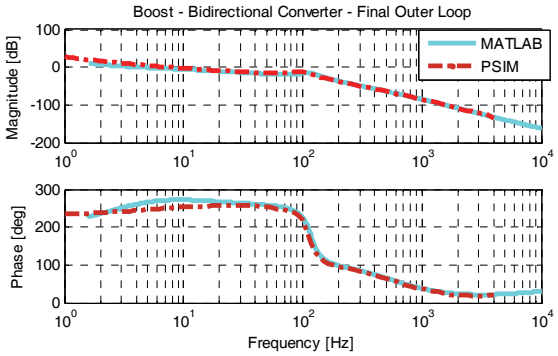

Fig. 14. The outer loop gain (T2) of the charger/discharger, including the output impedance of the boost converter (Solid: analytic, dotted: numerical result)

function, and the verification through numerical analysis.

Finally, the outer loop controller can be designed from the transfer function graph. As shown in Fig. 14, the phase margin of the outer-loop gain (T3) of the charger / discharger employing the design example of a PI controller is about 60°. The result confirms the stability of the feedback loop. From the results, it can be seen that all the MATLAB plots agree well with the simulation results of PSIM, which means that the transfer functions derived in the previous section are correct.

3. Experimental Results

This section describes the implementation of a 1 kW hardware prototype of the proposed standalone power conditioning system along with an energy storage subsystem, in order to verify the aforementioned analysis. Table I lists the element parameters concerning the hardware prototype. A TMS28335 (Texas Instrument) digital signal processor is used for the controller implementation. A couple of super-capacitor modules in series, each of which is 45V/41.7F (Nesscap Co.), are used for the energy storage device, to satisfy the higher voltage requirements of the proposed integrated system.

First, Fig. 15 shows that when the power from the renewable energy source is greater than the boost power to maintain the DC-link, the bi-directional converter (charger / discharger) automatically charges the energy storage. The figure also shows that the controller successfully

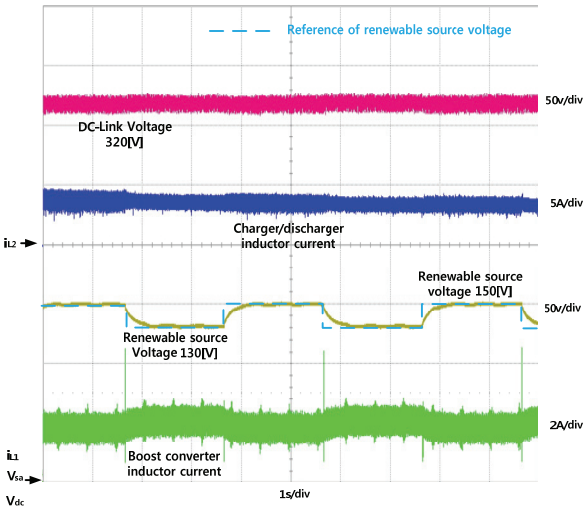

Fig. 15. Step response of output voltage of the renewable energy source and other key waveforms at charging mode (the arrows at left mean the ground).

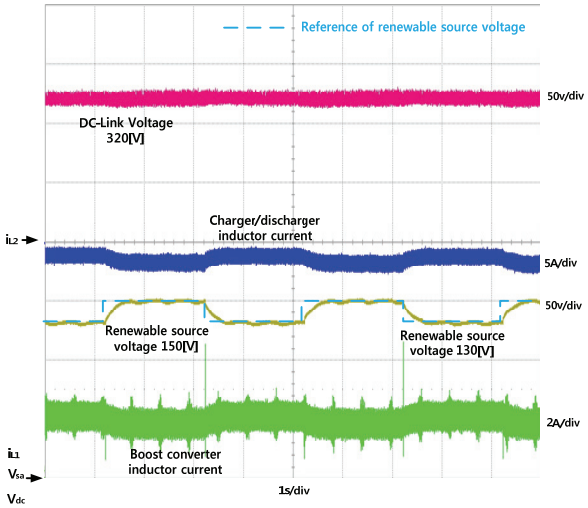

Fig. 16. Step response of output voltage of the renewable energy source and other key waveforms at dis-charg-ing mode.

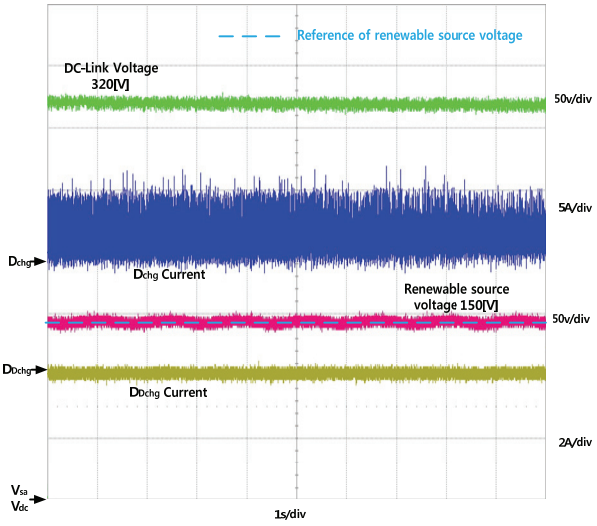

Fig. 17. Current waveforms of the charging diode (D_{Chg}) and discharging diode (D_{Dchg}), during the charging mode.

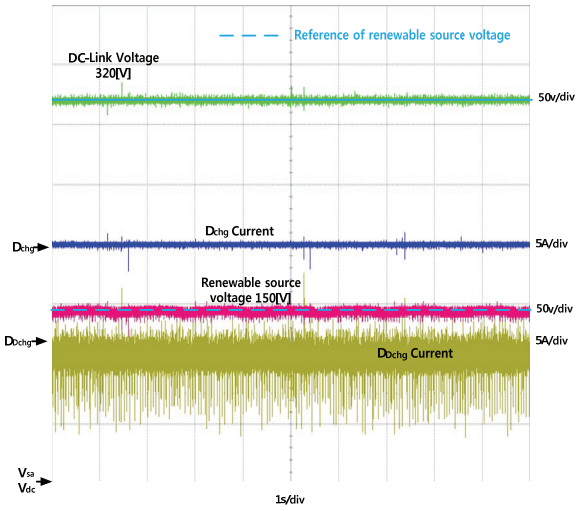

Fig. 18. Current of the charging diode (D_{Chg}) and dis-charging diode (D_{Dchg}), during the discharging mode.

controls the inductor current of the charger/discharger to regulate the DC-link voltage at 320V. Even when the voltage reference of the boost converter is step-changed periodically between 130V and 150V, the DC-link voltage is tightly regulated in the normal operation range. This case shows the good tracing capability and stability performance of the controller design.

Secondly, Fig. 16 shows that when the power generated from the energy source is lower than the power required to maintain the DC-link, the charger/discharger automatically discharges energy. The figure shows the controller still controls the inductor current of the charger/discharger well enough to regulate the DC-link voltage at 320V, while the reference of the boost converter is step-changed between 130V and 150V. This case also shows good tracing and stability performance.

Fig. 17 shows the current waveforms of the charging diode (D_{Chg}) and the discharging diode (D_{Dchg}), during the charging mode. Meanwhile, Fig. 18 shows the current waveforms of the charging diode (D_{Chg}) and discharging diode (D_{Dchg}) during the discharging mode. These figures demonstrate that the charging and discharging currents have different conduction paths from each other, as presented in \the operation principle of the proposed scheme (see Figs. 5 and 6).

4. Conclusion

This paper presents a new high efficiency power conditioning system together with an energy storage device. We perform dynamic response analysis for the design of the entire control scheme, including interaction modeling between the charger / discharger and main power stream. Then, we present the transfer function derivations for the DC-link regulation with a design example of the feedback controllers.

The power conditioning system of the renewable energy source together with an energy storage device achieves automatic, stable, and efficient operation of energy flow from the energy source, under standalone operation. We verify the transfer functions derived by the state-space averaging method by comparison between the numerical analysis using PSIM, and symbolic analysis of the averaged model with MATLAB.

Finally, we verify the analysis and design guidelines through the hardware experiment of a 1kW hardware prototype of a power conditioning system with an energy storage device.

Acknowledgement

This work was supported by the Human Resources Development Program (No. 20124030200070) of Korea Institute of Energy Technology Evaluation and Planning grant by the Korea Government Ministry of Knowledge Economy.

References

[1] Do-Hyun Kim, Jong-Ho Jang, Joung-Hu Park, Jung-Won Kim “Single-Ended High-Efficiency Step-up Converter Using the Isolated Switched-Capacitor Cell,” Journal of Power Electronics, Vol. 13, No. 5, pp. 766-778, Sept. 2013.

[2] Ahmet Teke, Mohammad Barghi Latran, Giovanni Spagnulolo, “Review of Multifunctional Inverter Topologies and Control Schemes Used in Distributed Generation Systems,” Journal of Power Electronics, pp. 324-340, Mar. 2013.

[3] Omran, W. A., Kazerani, M., Salama, M. M. A., “Investigation of Methods for Reduction of Power Fluctuations Generated From Large Grid-Connected Photovoltaic Systems”, Energy Conversion IEEE Transactions on, pp. 318-327, March 2011.

[4] Sun-Jae Park, Joung-Hu Park, Hee-Jong Jeon, “Controller design of grid-connected power conditioning system with energy storage device”, international conference on Electrical Machines and systems 2011, Beijing, China, 20-24 Aug. 2011.

[5] Sitterly, M., Le Yi Wang, Yin, G.G., Caisheng Wang, “Enhanced Identification of Battery Models for Real-Time Battery Management”, Sustainable Energy IEEE Transactions on, pp. 300-308, July 2011.

[6] Kakigano, H., Miura, Y., Ise, T., “Low-Voltage Bipolar-Type DC Microgrid for Super High Quality Distribution”, Power Electronics, IEEE Transactions on, pp. 3066-3075, Dec. 2010.

[7] Hongfei Wu, Runruo Chen, Junjun Zhang, Yan Xing, Haibing Hu, Hongjuan Ge, “A Family of Three-Port Half-Bridge Converters for a Standalone Renewable Power System”, Power Electronics IEEE Transactions on, pp. 2697-2706, Sept. 2011.

[8] Kai Sun, Li Zhang, Yan Xing, Guerrero, J.M., “A Distributed Control Strategy Based on DC Bus Signaling for Modular Photovoltaic Generation Systems with Battery Energy Storage”, Power Electronics, IEEE Transactions on, pp. 3032-3045, Oct. 2011.

[9] Yao, D.L., Choi, S.S., Tseng, K.J., Lie, T.T., “Determination of Short-Term Power Dispatch Schedule for a Wind Farm Incorporated with Dual-Battery Energy Storage Scheme”, Sustainable Energy IEEE Transactions on, pp. 74-84, Jan. 2012.

[10] Hao Qian, Jianhui Zhang, Jih-Sheng Lai, Wensong Yu, “A High-Efficiency Grid-Tie Battery Energy Storage System”, Power Electronics IEEE Transactions on, pp. 886-896, March 2011.

[11] Vilalva, M.G., de Siquerira, T.G., Ruppert, E., “Voltage regulation of photovoltaic arrays: small-signal analysis and control design” Power Electronics, IET, pp. 869-880, Nov. 2010.

[12] Barrade, P., Delalay, S., Rufer, A., “Direct Connec-

tion of Supercapacitors to Photovoltaic Panels With On-Off Maximum Power Point Tracking", Sustainable Energy, IEEE Transactions on, pp. 283-294, April 2012.
[13] J. H. Park, J. Y. Ahn, B. H. Cho and G. J. Yu, "Dual-Module-Based Maximum Power Tracking Control of Photovoltaic Systems," Industrial Electronics, IEEE Transaction on, Vol. 53, No. 4, AUG 2006, pp. 1036-1047.
[14] Minsoo Jang, Agelidis, V. G., "A Minimum Power-Processing-Stage Fuel-Cell Energy System Based on a Boost-Inverter with a Bidirectional Backup Battery Storage", Power Electronics IEEE Transactions on, pp. 1568-1577, May 2011.
[15] Maharjan, L., Yamagishi, T., Akagi, H., "Active-Power Control of Individual Converter Cells for a Battery Energy Storage System Based on a Multilevel Cascade PWM Converter", Power Electronics IEEE Transactions on, pp. 1099-1107, March 2012.
[16] Liming Liu, Hui Li, Zhichao Wu, Yan Zhou, "A Cascaded Photovoltaic System Integrating Segmented Energy Storages With Self-Regulating Power Allocation Control and Wide Range Reactive Power Compensation", Power Electronics, IEEE Transactions on, pp. 3545-3559, Dec. 2011.
[17] Aharon, I., Kuperman, A., "Topological Overview of Powertrains for Battery-Powered Vehicles with Range Extenders", Power Electronics IEEE Transactions on, pp. 868-876, March 2011.
[18] Zhongqiu Wang, Xi Li, Gengyin Li, Ming Zhou, Lo, K.L., "Energy storage control for the Photovoltaic generation system in a micro-grid", Critical Infrastructure (CRIS), 2010 5th International Conference on, pp. 1-5, Sept. 2010.
[19] Sérgio Augusto Oliveira da Silva, Pedro Francisco Donoso-Garcia, Porfirio Cabaleiro Cortizo, and Paulo Fernando Seixas, "A Three-Phase Line-Interactive UPS System Implementation With Series-Parallel Active Power-Line Conditioning Capabilities," IEEE Transactions on Industry Applications, vol. 38, no. 6, November/December 2002, pp. 1581-1590
[20] Zhi Jian Zhou, Xing Zhang, Po Xu, and Weixiang X. Shen, "Single-Phase Uninterruptible Power Supply Based on Z-Source Inverter," IEEE Transactions on Industrial Electronics, vol. 55, no. 8, august 2008, pp. 2997-3004.
[21] Chia-Chou Yeh, and Madhav D. Manjrekar, "A Reconfigurable Uninterruptible Power Supply System for Multiple Power Quality Applications," IEEE Transactions on Power Electronics, vol. 22, no. 4, JULY 2007, pp. 1361-1372.
[22] Sun-Jae Park, Hwa-Seok Lee, Chan-In Kim, Joung-Hu Park, Hee-Jong Jeon, and Jeongduk Ryeom, "Controller Design of a Novel Power Conditioning System with an Energy Storage Device forRenewable Energy Sources under Grid-Connected Operation," Journal of Power Electronics, Vol. 13, No. 3, May 2013, pp. 390-399.
[23] S. Makhloufi, R. Abdessemed, "Type-2 Fuzzy Logic Optimum PV/inverter Sizing Ratio for Grid-connected PV Systems," Journal of Electrical Engineering & Technology, Vol. 6, No. 6, Nov. 2011, pp. 731-741.
[24] Park, Sun-Jae, Mun, Sol, Park, Joung-Hu, Jeon, Hee-Jong, "Controller design of power conditioning systems with energy storage device for renewable energy source under standalone operation", Applied Power Electronics Conference and Exposition, pp. 1967-1972, Feb. 2012.

Sun-Jae Park received his B.S. and M.S. from the Department of Electrical Engineering of Soongsil University, Seoul, Korea, in 2009 and 2012, respectively. His current research interests include the analysis and design of high-frequency switching converters, etc.

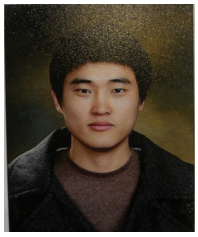

Jong-Hyun Shin received his B.S. from the Department of Electrical Engineering of Soongsil University, Seoul, Korea, in 2013. He is currently a master student at Soongsil University, Seoul, Korea. His current research interests include the analysis and design of bi-directional switching converters, etc.

Joung-Hu Park received his B.S., M.S. and Ph.D. from the Department of Electrical Engineering and Computer Science of Seoul National University, Seoul, Korea, in 1999, 2001 and 2006, respectively. He is currently an Assistant Professor at Soongsil University, Seoul, Korea. His current research interests include the analysis of high-frequency switching converters and renewable energy applications, etc.

Hee-Jong Jeon received his B.S. from Soongsil University, Seoul, Korea, his M.S. from Seoul National University, Seoul, Korea, and his Ph.D. from Chung-Ang University, Seoul, Korea, in 1975, 1977 and 1987, respectively. He was a Vice President of the Korea Institute of Power Electronics from 2000 to 2001. He is currently a Professor at Soongsil University, Seoul, Korea. His current research interests include mechatronics systems, automation control and renewable energy systems, etc.